HOKKAIDO UNIVERSITY

Title	Essential role of the cytochrome P450 CYP4F22 in the production of acylceramide, the key lipid for skin permeability barrier formation
Author(s)	Ohno, Yusuke; Nakamichi, Shota; Ohkuni, Aya et al.
Citation	Proceedings of the National Academy of Sciences, 112(25), 7707-7712 https://doi.org/10.1073/pnas.1503491112
Issue Date	2015-06-23
Doc URL	https://hdl.handle.net/2115/60363
Type	journal article
File Information	manuscript.pdf

Hokkaido University Collection of Scholarly and Academic Papers : HUSCAP

Essential role of the cytochrome P450 CYP4F22 in the production of acylceramide, the key lipid for skin permeability barrier formation

Yusuke Ohno[a], Shota Nakamichi[a], Aya Ohkuni[a], Nozomi Kamiyama[a], Ayano Naoe[b], Hisashi Tsujimura[b], Urara Yokose[b], Kazumitsu Sugiura[c], Junko Ishikawa[b], Masashi Akiyama[c], and Akio Kihara[a,1]

[a]Laboratory of Biochemistry, Faculty of Pharmaceutical Sciences, Hokkaido University, Kita 12-jo, Nishi 6-chome, Kita-ku, Sapporo 060-0812, Japan; [b]Kao Corporation, 2606, Akabane, Ichikai-Machi, Haga-gun, Tochigi 321-3497, Japan; and [c]Department of Dermatology, Nagoya University Graduate School of Medicine, 65 Tsurumai-cho, Showa-ku, Nagoya 466-8550, Japan

[1]To whom correspondence should be addressed:

Akio Kihara

Laboratory of Biochemistry, Faculty of Pharmaceutical Sciences

Hokkaido University

Kita 12-jo, Nishi 6-chome, Kita-ku, Sapporo 060-0812, Japan

Tel: +81-11-706-3754

Fax: +81-11-706-4900

E-mail: kihara@pharm.hokudai.ac.jp

Short title: Skin barrier formation by CYP4F22

Abstract

A skin permeability barrier is essential for terrestrial animals, and its impairment causes several cutaneous disorders such as ichthyosis and atopic dermatitis. Although acylceramide is an important lipid for the skin permeability barrier, details of its production have yet to be determined, leaving the molecular mechanism of skin permeability barrier formation unclear. Here we identified the cytochrome P450 gene *CYP4F22* as the long-sought fatty acid ω-hydroxylase gene required for acylceramide production. *CYP4F22* has been identified as one of the autosomal recessive congenital ichthyosis-causative genes. Ichthyosis mutant proteins exhibited reduced enzyme activity, indicating correlation between activity and pathology. Furthermore, lipid analysis of an ichthyosis patient showed a drastic decrease in acylceramide production. We determined that CYP4F22 was a type I membrane protein that locates in the endoplasmic reticulum (ER), suggesting that the ω-hydroxylation occurs on the cytoplasmic side of the ER. The preferred substrate of the CYP4F22 was ≥C28 fatty acids. In conclusion, our findings demonstrated that CYP4F22 is an ultra long-chain fatty acid ω-hydroxylase responsible for acylceramide production and provides important new insights into the molecular mechanisms of skin permeability barrier formation. Furthermore, based on the results obtained here, we proposed a detailed reaction series for acylceramide production.

Keywords: acylceramide; ceramide; lipid; skin; sphingolipid

Significance statement

The sphingolipid backbone ceramide is the major lipid species in the stratum corneum and plays a pivotal function in skin permeability barrier formation. Acylceramide is an important epidermis-specific ceramide species. However, the details of acylceramide production including its synthetic genes, reactions and their orders, and intracellular site for production, have remained unclear. In the present study, we identified the cytochrome P450 CYP4F22 as the missing fatty acid ω-hydroxylase required for acylceramide synthesis. We also determined that CYP4F22 is a type I ER membrane protein and that its substrate is ultra long-chain fatty acids. Our findings provide important new insights into the molecular mechanisms of not only acylceramide production but also skin permeability barrier formation.

Introduction

A skin permeability barrier protects terrestrial animals from inside the body, penetration of external soluble materials, and infection by pathogenetic organisms. In the stratum corneum, the outermost cell layer of the epidermis, multiple lipid layers (lipid lamellae) play a pivotal function in barrier formation (Fig. S1) (1-3). Impairment of the skin permeability barrier leads to several cutaneous disorders, such as ichthyosis, atopic dermatitis, and infectious diseases.

The major components of the lipid lamellae are ceramide (the sphingolipid backbone), cholesterol, and free fatty acid (FA). In most tissues, ceramide consists of a long-chain base (LCB; usually sphingosine) and an amide-linked FA with a chain length of 16-24 (C16-C24) (4, 5). On the other hand, ceramide species in the epidermis are strikingly unique (Fig. S2*A*). For example, epidermal ceramides contain specialized LCBs (phytosphingosine and 6-hydroxysphingosine) and/or FAs with α- or ω-hydroxylation (1-3). In addition, substantial amounts of epidermal ceramides have ultra long-chain (ULC) FAs (ULCFAs) with ≥C26 (4, 5). The most unique epidermal ceramides are acylceramides having C28-C36 ULCFAs, which are ω-hydroxylated and esterified with linoleic acid (EOS in Fig. S1; EODS, EOS, EOP, and EOH in Fig. S2*A*) (1-3, 6, 7). These characteristic molecules may be important to increase the hydrophobicity of lipid lamellae and/or to stabilize the multiple lipid layers. Linoleic acid is one of the essential FAs, and its deficiency causes ichthyosis symptoms due to a failure to form normal acylceramide (8). Ichthyosis is a cutaneous disorder accompanied by dry, thickened, and scaly skin; it is caused by a barrier abnormality. In atopic dermatitis patients, both total ceramide levels and the chain length of ceramides are decreased, and ceramide composition is also altered (9-11).

In addition to its essential function in the formation of lipid lamellae, acylceramide is also important as a precursor of protein-bound ceramide, which functions to connect lipid lamellae and corneocytes (Fig. S1) (12, 13). After removal of linoleic acid, the exposed ω-hydroxyl group of acylceramide is covalently bound to corneocyte proteins, forming a corneocyte lipid envelope. Acylceramides and protein-bound ceramides are important in epidermal barrier formation, and mutations in the genes involved in their synthesis, including *CERS3*, *ALOX12B*, and *ALOXE3*, can cause non-syndromic, autosomal recessive congenital ichthyosis (ARCI) (3, 14-16). The ceramide synthase CERS3 catalyzes the amide bond formation between an LCB base and ULCFA, producing ULC-ceramide, which is the precursor of acylceramide (Fig. S1 and Fig. S2*B*) (17). The 12(*R*)-lipoxygenase ALOX12B and epidermal lipoxygenase-3 ALOXE3 are required for the formation of protein-bound ceramides (13, 18). Other ARCI genes include the ATP-binding cassette (ABC) transporter *ABCA12*, the transglutaminase *TGM1*, *NIPAL4*/*ICHTHYIN*, *CYP4F22*/*FLJ39501*, *LIPN*, and *PNPLA1* (16, 19). The exact functions of *NIPAL4*, *LIPN*, and *PNPLA1* are currently unclear. Causative genes of syndromic forms of ichthyosis also include a gene required for acylceramide synthesis: the FA elongase *ELOVL4*, which produces ULCFA-CoAs, the substrate of CERS3 (20).

Although acylceramide is essential for the epidermal barrier function, the mechanism behind acylceramide production is still poorly understood, leaving the molecular mechanisms behind epidermal barrier formation unclear. For example, acylceramide production requires ω-hydroxylation of the FA moiety of ceramide. However, the ω-hydroxylase responsible for this reaction has been heretofore unidentified (Fig. S1). Here, we identified the cytochrome P450 CYP4F22, also known as FLJ39501, as this missing FA ω-hydroxylase required for acylceramide production. *CYP4F22* had been identified as one of the ARCI genes (21),

although its function in epidermal barrier formation remained unsolved. Our findings clearly demonstrate a relationship between ARCI pathology, acylceramide levels, and ω-hydroxylase activity.

Results

Identification of CYP4F22 as the FA ω-Hydroxylase Required for ω-Hydroxyceramide Production

Although researchers have long known ω-hydroxylation is essential for acylceramide formation, they have long puzzled over which gene is responsible for this reaction. To identify this gene, we first established a cell system that produced ULC-ceramides, a possible substrate of interest for ω-hydroxylase, since most cells cannot produce such extremely long ceramides. Human embryonic kidney (HEK) 293T cells overproducing the FA elongase ELOVL4 and/or the ceramide synthase CERS3 were labeled with [^{3}H]sphingosine, and the chain lengths of ceramides were determined by reverse-phase thin-layer chromatography (TLC). Although overexpression of either ELOVL4 or CERS3 alone did not result in the production of ULC-ceramides, their co-overproduction caused generation of ULC-ceramides with ≥C26 (Fig. 1*A*). They migrated slower than long-chain (LC; C16-C20) ceramides and very long-chain (VLC; C22-C24) ceramides on reverse-phase TLC. Production of ULC-ceramides with chain length up to C36 was also confirmed by liquid chromatography-mass spectrometry (LC-MS) analysis (Fig. S3). When labeled lipids were separated by normal-phase TLC, ULC-ceramides were detected as a band at the adjacent, upper position of VLC-ceramides (Fig. 1*B*).

It has been reported that the cytochrome P450 (CYP) inhibitor aminobenzotriazole inhibits the generation of ω-hydroxyceramide in cultured human keratinocytes (22). In humans, 57 *CYP* genes exist, and mammalian *CYP* genes are classified into 18 families and 43 subfamilies. Some CYP4F members are implicated in the ω-hydroxylation of long-chain FAs (23, 24), raising the possibility that certain CYP4F subfamily members are responsible for ω-hydroxylation of ULCFAs in acylceramide formation. To test this possibility, we

cloned all of the human *CYP4F* subfamily genes (*CYP4F2*, *3A*, *3B*, *8*, *11*, *12*, and *22*), and each was expressed as an N-terminally 3xFLAG-tagged protein in HEK 293T cells overproducing 3xFLAG-ELOVL4 and 3xFLAG-CERS3. All CYP4F subfamily proteins were expressed at similar levels (Fig. 2*A*). Among the CYP4F subfamily members, only CYP4F22 caused the disappearance of ULC-ceramide, which was concomitant with the production of a new band at the position of ω-hydroxyceramide (Fig. 2*B* and Fig. S4). LC-MS analysis determined that this band indeed represented ω-hydroxyceramides with C28-C36 (Fig. S5). Thus, CYP4F22 is the ω-hydroxylase required for ω-hydroxyceramide production.

Correlation between CYP4F22 Activity and Ichthyosis Pathology

Although *CYP4F22* gene has been identified as one of the ARCI-causative genes (21, 25), its function in epidermal barrier formation has remained unsolved. Five missense mutations, which all cause amino acid substitutions (F59L, R243H, R372W, H435Y, and H436D), have been found in the *CYP4F22* of ichthyosis patients. To examine their role in ichthyosis pathology, we introduced these mutations into *CYP4F22* and examined the ω-hydroxylase activity of the resultant mutant proteins. All mutant proteins were expressed at equivalent levels to the wild type protein (Fig. 3*A*), and indeed all ω-hydroxylase activity of the mutant CYP4F22 proteins decreased to 4-20% of wild type protein activity (Fig. 3*B*). Therefore, protein activity and ichthyosis pathology were nicely correlated.

That being noted, ichthyosis due to *CYP4F22* mutation is quite rare. In fact, a mere ~20 patients have been reported in Mediterranean populations (21), and only a single patient in Japan (25). The Japanese patient has compound heterozygous *CYP4F22* mutations: one is a point mutation (c.728G>A) causing amino acid substitution (p.R243H; R243H) and the other

is a deletion (c.1138delG) causing a frame shift (p.D380TfsX2; D380TfsX2), in which Asp380 is substituted to Thr followed by a stop codon (25). The mutant R243H exhibited the decreased activity as described above (Fig. 3*B*). We also introduced the c.1138delG mutation into *CYP4F22* and examined the ω-hydroxylase activity of its truncated protein product. D380TfsX2 (predicted molecular mass, 44.8 kDa) migrated faster than the wild type protein (62.0 kDa, Fig. 3*A*), and we found that it exhibited no activity (Fig. 3*B*).

To confirm our conclusion that CYP4F22 is involved in the production of acylceramide through ω-hydroxyceramide synthesis, we subjected the stratum corneum of the Japanese patient (Fig. 3*C*), as well as those of controls (her parents and a healthy volunteer), to LC-MS analysis and examined the levels of 11 major ceramide species. Although statistical analysis could not be performed due to the low number of samples, all three acylceramides containing sphingosine (EOS), 6-hydroxysphingsoine (EOH), and phytosphingosine (EOP) were apparently decreased in the ARCI patient compared to the controls (to <1/10) (Fig. 3*D* and Table S1). Instead, the non-acylated ceramides NS (which are a combination of sphingosine and a non-hydroxylated FA) and AS (which are a combination of sphingosine and an α-hydroxylated FA) seemed to be increased (Table S1). These results confirm that ω-hydroxyceramide production by CYP4F22 is indeed required for acylceramide synthesis.

CYP4F22 Is a Type I Endoplasmic Reticulum Membrane Protein

We next examined the subcellular localization of CYP4F22 by subjecting 3xFLAG-tagged CYP4F22 to indirect immunofluorescence microscopy (Fig. 4*A*). 3xFLAG-CYP4F22 exhibited a reticular localization pattern and was co-localized with calnexin, HA-ELOVL4, and HA-CERS3, all of which are endoplasmic reticulum (ER) proteins, indicating CYP4F22 is localized in the ER. A hydropathy plot showed that CYP4F22 contains a highly

hydrophobic region at the N-terminus as well as some weak hydrophobic stretches (Fig. 4*B*). To reveal the membrane topology of CYP4F22, we introduced a *N*-glycosylation cassette, which is *N*-glycosylated when exposed to the lumen of the ER, into several positions of CYP4F22, the N-terminus, E85/K (between Glu85 and Lys86 residues), H155/R, A285/L, C361/R, D455/N, and R508/K. Among these fusion proteins, only CYP4F22 containing the *N*-glycosylation cassette at the N-terminus received glycosylation, as the molecular weight shift was observed upon treatment with endoglycosidase H (Fig. 4*C*). This result indicates that CYP4F22 spans the ER membrane once. Furthermore, it oriented its N-terminus to the ER lumen and the large, hydrophilic C-terminal domain containing the active site to the cytosolic side of the ER membrane. The same membrane topology was determined for other CYP members by the detection of N-terminal *N*-glycosylation (26, 27).

When the N-terminal hydrophobic region was removed, the resulting CYP4F22ΔN became distributed throughout the cytoplasm (Fig. 4*D*). CYP4F22ΔN was fractionated into both the soluble and membrane fractions by ultracentrifugation, in contrast to full-length CYP4F22, which was detected only in the membrane fraction (Fig. 4*E*). These results confirmed that CYP4F22 is a type I ER membrane protein. CYP4F22ΔN could not produce ω-hydroxyceramide (Fig. 4*F*), suggesting that anchoring to the ER membrane, where all of the reactions of acylceramide synthesis occur, is crucial for the CYP4F22 function.

ULCFAs Are Substrates of CYP4F22

It was still unclear whether CYP4F22 introduces a ω-hydroxyl group into ULCFAs before or after formation of ceramide. Therefore, we examined ω-hydroxy FA levels using LC-MS in the presence of the ceramide synthase inhibitor fumonisin B_1. If ω-hydroxylation occurs prior to ceramide production, it was expected that free ω-hydroxy FA levels should be increased

with fumonisin B_1 treatment. We found that ω-hydroxy FA levels with C26-C36 were significantly increased by addition of fumonisin B_1 (Fig. 5*A*), suggesting that ω-hydroxylation occurs prior to ceramide production. Thus, it is highly likely that the substrates of CYP4F22 are not ceramides but rather FAs, the same type of substrate as catalyzed by other CYP4F family members.

To confirm that the substrates of CYP4F22 are FAs, we performed an *in vitro* analysis utilizing yeast, which has no endogenous FA ω-hydroxylase activity. When C30:0 FA was used as a substrate, the total membrane fractions prepared from yeast bearing a vector plasmid exhibited FA ω-hydroxylase activity only at the background levels (Fig. 5*B*). On the other hand, the ectopic expression of human CYP4F22 resulted in the production of ω-hydroxy FA in an NADPH-dependent manner (Fig. 5*B*). The hydroxylation reactions by CYP generally require O_2 and NADPH. These results indicated that the substrates of CYP4F22 are indeed FAs.

Acylceramide specifically contains ULCFA (mostly C28-C36) as its FA component. It is possible that the substrate preference of CYP4F22 determines the FA chain length of acylceramides. To examine this possibility, we prepared HEK 293T cells producing different sets of ceramides with specific chain lengths by introducing particular combinations of ceramide synthase and FA elongase (ELOVL1 and CERS2, C22-C24 ceramides; ELOVL1 and CERS3, C26 ceramide; and ELOVL4 and CERS3, ≥C26 ceramides) (Fig. 5*C*) (28, 29). Mammals have six ceramide synthases (CERS1-6) and seven FA elongases (ELOVL1-7), and each exhibits characteristic substrate specificity (Fig. S2*B*) (2, 4, 5, 28). When CYP4F22 was expressed in these cells producing different ceramide species, ω-hydroxyceramides were produced in cells producing C26 ceramide (ELOVL1/CERS3 combination) and ≥C26 ceramides (ELOVL4/CERS3 combination) but not in cells producing C22-C24 ceramides

(ELOVL1/CERS2 combination) (Fig. 5*D*). These results suggest that CYP4F22 can ω-hydroxylate ULCFAs (≥C26) but not VLCFAs (C22 and C24). The levels of ω-hydroxyceramide produced in ELOVL1/CERS3 cells were similar to those in ELOVL4/CERS3 cells, although the levels of non-hydroxyceramide substrates were much higher in ELOVL1/CERS3 cells. Thus, CYP4F22 exhibits especially high activity toward ULCFAs with ≥C28.

Discussion

Here we identified CYP4F22 as an ULCFA ω-hydroxylase involved in acylceramide production. Acylceramide is quite important for epidermal barrier formation, and impairment of its production such as by *ELOVL4* and *CERS3* mutations causes ichthyosis (15, 20). *CYP4F22* was first identified as an ARCI-causative gene by Fischer and her co-workers (21). They proposed that CYP4F22 and most other ichthyosis-causative genes are involved in a metabolic pathway producing 12-lipoxygenase products (hepoxilins and trioxilins) from arachidonic acid by analogy to the 5-lipoxygease pathway creating leukotrienes. In their scenario, arachidonic acid is first converted to 12(*R*)-hydroperoxyeicosatetraenoic acid (12(*R*)-HPETE) by one of the ichthyosis gene products, ALOX12B, and then to 12(*R*)-hepoxilin A_3 by another ichthyosis gene product, ALOXE3. 12(*R*)-Hepoxilin A_3 is further converted to a triol compound, 12(*R*)-trioxilin A_3. CYP4F22 was proposed to be involved in the metabolism of 12(*R*)-trioxilin A_3 by converting 12(*R*)-trioxilin A_3 to 20-hydroxy-12(*R*)-trioxilin A_3. However, the exact roles of hepoxilins and trioxilins in epidermal barrier formation and/or keratinocyte differentiation are still unclear. Furthermore, recent findings demonstrated that ALOX12B and ALOXE3 are rather involved in the reactions necessary for conversion of acylceramide to protein-bound ceramide, *i.e.*, peroxidation of the linoleate moiety and subsequent epoxyalcohol derivatization (13). In addition, ALOX12B was proven not to be involved in hepoxilin/trioxilin production (30). These findings suggested that while hepoxilin/trioxilin metabolism may not be relevant to the pathogenesis of ichthyosis, the impairment of acylceramide/protein-bound ceramide formation causes ichthyosis. Based on these recent findings, some researchers have predicted that CYP4F22 is involved in acylceramide generation (3, 31), but their suppositions have lacked experimental evidence — until now.

We determined the membrane topology of CYP4F22 (Fig. 4*C*), which indicates that the large C-terminal hydrophilic domain including catalytic residues is located in the cytosol. Therefore, ω-hydroxylation of the ULCFA portion of acylceramide must occur on the cytosolic side of the ER membrane. Based on this finding, we propose a working model for the process of acylceramide production in the ER membrane as follows (Fig. S6). Elongation of palmitoyl-CoA to ULCFA-CoA occurs on the cytoplasmic side of the ER membrane. Since lipids comprising the ER membrane are mostly C16 and C18, ULCFA (C28-C36) portions of ULCFA-CoAs should be bent in the cytosolic leaflet of the ER membrane (Fig. S6) or be penetrated into the luminal leaflet. Although the latter possibility cannot be excluded, we prefer the former possibility, since in the latter model ULCFA must 'flip-flop' at least three times in the ER membrane in the course of acylceramide production. Since the substrates of CYP4F22 are ULCFAs (Fig. 5), ULCFA-CoAs should be converted to ULCFAs before ω-hydroxylation. After ω-hydroxylation of ULCFAs by CYP4F22, the resulting ω-hydroxy-ULCFA is converted to ω-hydroxy-ULCFA-CoA by acyl-CoA synthetase. ACSVL4/FATP4 is the candidate acyl-CoA synthetase for this reaction, since *Acsvl4* mutant mice exhibited skin barrier defects (32). CERS3 catalyzes formation of ω-hydroxyceramide from ω-hydroxy-ULCFA-CoA and LCB. An unknown acyltransferase then introduces linoleic acid into the ω-hydroxy group of ω-hydroxyceramide, generating acylceramide.

Our results presented here demonstrated for the first time that CYP4F22 is a *bona fide* ULCFA ω-hydroxylase required for acylceramide production. Our findings provide important new insights into the molecular mechanisms of skin permeability barrier formation. Future development of compounds that strengthen the skin permeability barrier by increasing acylceramide-synthetic proteins such as ELOVL4, CERS3, and CYP4F22 may be useful for treatment of cutaneous disorders including ichthyosis and atopic dermatitis.

Materials and Methods

Detailed materials and methods used for all procedures are available in *SI* Text.

[^{3}H]Sphingosine Labeling assay

Cells were labeled with 2 μCi [3-^{3}H]sphingosine (20 Ci/mmol; PerkinElmer Life Sciences, Waltham, MA) for 4 h at 37 °C. Lipids were extracted as described previously (28, 33) and separated by normal-phase TLC and reverse-phase TLC.

Lipid Analysis Using LC-MS

FAs and ceramides prepared from cultured cells were analyzed by reversed-phase LC/MS using ultra-performance liquid chromatography (UPLC) coupled with electrospray ionization (ESI) tandem triple quadrupole MS (Xevo TQ-S; Waters, Milford, MA). FAs were analyzed after derivatization to *N*-(4-aminomethylphenyl)pyridinium (AMPP) amides using the AMP$^+$ Mass Spectrometry Kit (Cayman Chemical, Ann Arbor, MI). Stratum corneum ceramides were analyzed by reversed-phase LC/MS using Agilent 1100 Series LC/MSD SL system (Agilent Technologies, Santa Clara, CA).

Immunoblotting

Immunoblotting was performed as described previously (34, 35) using anti-FLAG M2 (1.85 μg/mL; Sigma, St. Louis, MO), anti-calnexin 4F10 (1 μg/mL; Medical & Biological Laboratories, Aichi, Japan), or anti-GAPDH 6C5 (1 μg/mL; Ambion, Life Technologies, Carlsbad, CA) antibody as a primary antibody and an HRP-conjugated anti-mouse IgG F(ab')$_2$ fragment (1:7500 dilution; GE Healthcare Life Sciences, Buckinghamshire, UK) as a

secondary antibody. Labeling was detected using Pierce ECL Western Blotting Substrate (Thermo Fisher Scientific, Waltham, MA).

Footnotes

Y.O. designed and performed the experiments and analyzed the data. S.N., A.O., and N.K. performed the experiments. K.S. and M.A. prepared stratum corneum samples from controls and an ARCI patient, and A.N., H.T., U.Y., and J.I. analyzed their ceramide compositions. A.K. planned the project, designed the experiments, and wrote the manuscript.

The authors declare no conflict of interest.

Acknowledgments

This work was supported by the Creation of Innovation Centers for Advanced Interdisciplinary Research Areas Program (to A.K.) from the Ministry of Education, Culture, Sports, Science and Technology of Japan; a Grant-in-Aid for Scientific Research (A) 26251010 (to A.K.); and a Grant-in-Aid for Young Scientists (A) 15H05589 (to Y.O.), both from the Japan Society for the Promotion of Science.

References

1. Uchida Y, Holleran WM (2008) Omega-O-acylceramide, a lipid essential for mammalian survival. *J Dermatol Sci* 51(2):77-87.
2. Mizutani Y, Mitsutake S, Tsuji K, Kihara A, Igarashi Y (2009) Ceramide biosynthesis in keratinocyte and its role in skin function. *Biochimie* 91(6):784-790.
3. Breiden B, Sandhoff K (2014) The role of sphingolipid metabolism in cutaneous permeability barrier formation. *Biochim Biophys Acta* 1841(3):441-452.
4. Kihara A (2012) Very long-chain fatty acids: elongation, physiology and related disorders. *J Biochem* 152(5):387-395.
5. Sassa T, Kihara A (2014) Metabolism of very long-chain fatty acids: genes and pathophysiology. *Biomol Ther* 22(2):83-92.
6. Farwanah H, Wohlrab J, Neubert RH, Raith K (2005) Profiling of human stratum corneum ceramides by means of normal phase LC/APCI-MS. *Anal Bioanal Chem* 383(4):632-637.
7. Masukawa Y, et al. (2008) Characterization of overall ceramide species in human *stratum corneum*. *J Lipid Res* 49(7):1466-1476.
8. Wertz PW, Cho ES, Downing DT (1983) Effect of essential fatty acid deficiency on the epidermal sphingolipids of the rat. *Biochim Biophys Acta* 753(3):350-355.
9. Imokawa G, et al. (1991) Decreased level of ceramides in stratum corneum of atopic dermatitis: an etiologic factor in atopic dry skin? *J Invest Dermatol* 96(4):523-526.
10. Ishikawa J, et al. (2010) Changes in the ceramide profile of atopic dermatitis patients. *J Invest Dermatol* 130(10):2511-2514.

11. Janssens M, et al. (2012) Increase in short-chain ceramides correlates with an altered lipid organization and decreased barrier function in atopic eczema patients. *J Lipid Res* 53(12):2755-2766.

12. Wertz PW, Downing DT (1987) Covalently bound ω-hydroxyacylsphingosine in the stratum corneum. *Biochim Biophys Acta* 917(1):108-111.

13. Zheng Y, et al. (2011) Lipoxygenases mediate the effect of essential fatty acid in skin barrier formation: a proposed role in releasing omega-hydroxyceramide for construction of the corneocyte lipid envelope. *J Biol Chem* 286(27):24046-24056.

14. Jobard F, et al. (2002) Lipoxygenase-3 (*ALOXE3*) and 12(*R*)-lipoxygenase (*ALOX12B*) are mutated in non-bullous congenital ichthyosiform erythroderma (NCIE) linked to chromosome 17p13.1. *Hum Mol Genet* 11(1):107-113.

15. Eckl KM, et al. (2013) Impaired epidermal ceramide synthesis causes autosomal recessive congenital ichthyosis and reveals the importance of ceramide acyl chain length. *J Invest Dermatol* 133(9):2202-2211.

16. Traupe H, Fischer J, Oji V (2014) Nonsyndromic types of ichthyoses - an update. *J Dtsch Dermatol Ges* 12(2):109-121.

17. Jennemann R, et al. (2012) Loss of ceramide synthase 3 causes lethal skin barrier disruption. *Hum Mol Genet* 21(3):586-608.

18. Krieg P, Furstenberger G (2014) The role of lipoxygenases in epidermis. *Biochim Biophys Acta* 1841(3):390-400.

19. Akiyama M, Shimizu H (2008) An update on molecular aspects of the non-syndromic ichthyoses. *Exp Dermatol* 17(5):373-382.

20. Aldahmesh MA, et al. (2011) Recessive mutations in *ELOVL4* cause ichthyosis, intellectual disability, and spastic quadriplegia. *Am J Hum Genet* 89(6):745-750.

21. Lefevre C, et al. (2006) Mutations in a new cytochrome P450 gene in lamellar ichthyosis type 3. *Hum Mol Genet* 15(5):767-776.

22. Behne M, et al. (2000) Omega-hydroxyceramides are required for corneocyte lipid envelope (CLE) formation and normal epidermal permeability barrier function. *J Invest Dermatol* 114(1):185-192.

23. Dhar M, Sepkovic DW, Hirani V, Magnusson RP, Lasker JM (2008) Omega oxidation of 3-hydroxy fatty acids by the human CYP4F gene subfamily enzyme CYP4F11. *J Lipid Res* 49(3):612-624.

24. Sanders RJ, Ofman R, Dacremont G, Wanders RJ, Kemp S (2008) Characterization of the human ω-oxidation pathway for ω-hydroxy-very-long-chain fatty acids. *FASEB J* 22(6):2064-2071.

25. Sugiura K, et al. (2013) Lamellar ichthyosis in a collodion baby caused by *CYP4F22* mutations in a non-consanguineous family outside the Mediterranean. *J Dermatol Sci* 72(2):193-195.

26. Szczesna-Skorupa E, Kemper B (1993) An N-terminal glycosylation signal on cytochrome P450 is restricted to the endoplasmic reticulum in a luminal orientation. *J Biol Chem* 268(3):1757-1762.

27. Shimozawa O, et al. (1993) Core glycosylation of cytochrome P-450(arom). Evidence for localization of N terminus of microsomal cytochrome P-450 in the lumen. *J Biol Chem* 268(28):21399-21402.

28. Ohno Y, et al. (2010) ELOVL1 production of C24 acyl-CoAs is linked to C24 sphingolipid synthesis. *Proc Natl Acad Sci USA* 107(43):18439-18444.

29. Sassa T, et al. (2013) Impaired epidermal permeability barrier in mice lacking *Elovl1*, the gene responsible for very-long-chain fatty acid production. *Mol Cell Biol* 33(14):2787-2796.

30. Krieg P, et al. (2013) *Aloxe3* knockout mice reveal a function of epidermal lipoxygenase-3 as hepoxilin synthase and its pivotal role in barrier formation. *J Invest Dermatol* 133(1):172-180.

31. Elias PM, et al. (2014) Formation and functions of the corneocyte lipid envelope (CLE). *Biochim Biophys Acta* 1841(3):314-318.

32. Moulson CL, et al. (2003) Cloning of wrinkle-free, a previously uncharacterized mouse mutation, reveals crucial roles for fatty acid transport protein 4 in skin and hair development. *Proc Natl Acad Sci USA* 100(9):5274-5279.

33. Nakahara K, et al. (2012) The Sjögren-Larsson syndrome gene encodes a hexadecenal dehydrogenase of the sphingosine 1-phosphate degradation pathway. *Mol Cell* 46(4):461-471.

34. Kihara A, et al. (2003) Sphingosine-1-phosphate lyase is involved in the differentiation of F9 embryonal carcinoma cells to primitive endoderm. *J Biol Chem* 278(16):14578-14585.

35. Kitamura T, Takagi S, Naganuma T, Kihara A (2015) Mouse aldehyde dehydrogenase ALDH3B2 is localized to lipid droplets via two C-terminal tryptophan residues and lipid modification. *Biochem J* 465(1):79-87.

Figure Legends

Fig. 1. Overproduction of ELOVL4 and CERS3 causes generation of ULC-ceramides. HEK 293T cells were transfected with plasmids encoding *3xFLAG-ELOVL4* and *3xFLAG-CERS3*, as indicated. Cells were labeled with [^{3}H]sphingosine for 4 h at 37 °C. Lipids were extracted, separated by reverse-phase TLC (*A*) or normal-phase TLC (*B*), and detected by autoradiography. Cer, ceramide; GlcCer, glucosylceramide; SPH, sphingosine; SM, sphingomyelin.

Fig. 2. CYP4F22 is involved in ω-hydroxyceramide synthesis. HEK 293T cells were transfected with plasmids encoding *3xFLAG-ELOVL4*, *3xFLAG-CERS3*, and *3xFLAG-CYP4F* subfamily members, as indicated. (*A*) Total lysates prepared from the transfected cells were separated by SDS-PAGE, followed by immunoblotting with anti-FLAG antibodies. (*B*) Cells were labeled with [^{3}H]sphingosine for 4 h at 37 °C. Lipids were extracted, separated by normal-phase TLC, and detected by autoradiography. Cer, ceramide; GlcCer, glucosylceramide; SPH, sphingosine; SM, sphingomyelin; ω-OH, ω-hydroxy.

Fig. 3. Hydroxylase activity of CYP4F22 is impaired by ichthyosis-causing mutations. (*A* and *B*) HEK 293T cells were transfected with plasmids encoding *3xFLAG-ELOVL4*, *3xFLAG-CERS3*, and *3xFLAG-CYP4F22* (wild type (WT) or mutant), as indicated. (*A*) Total cell lysates prepared from the transfected cells were separated by SDS-PAGE and subjected to immunoblotting with anti-FLAG antibodies. (*B*) The transfected cells were labeled with [^{3}H]sphingosine for 4 h at 37 °C. Extracted lipids were separated by normal-phase TLC and detected by autoradiography. Cer, ceramide; GlcCer, glucosylceramide; SPH, sphingosine; SM, sphingomyelin; ω-OH, ω-hydroxy. (*C*) Representative clinical feature of an ARCI

patient (at 2 years old). Leaf-like flakes presented on the extensor side of the left lower limb prior to tape stripping. (*D*) Acylceramide (EOS, EOH, and EOP) levels in stratum corneum of a control (WT/WT), carriers (WT/R243H, ichthyosis patient's father; WT/D380T fs2X (fs2X), patient's mother), and an ARCI patient (R243H/D380T fs2X) were measured by LC-MS.

Fig. 4. CYP4F22 is a type I ER membrane protein. (*A*, *D*, and *E*) HeLa cells were transfected with plasmids encoding *HA-ELOVL4*, *HA-CERS3*, *3xFLAG-CYP4F22*, and *3xFLAG-CYP4F22ΔN* (CYP4F22 lacking 54 N-terminal amino acids), as indicated. (*A* and *D*) Cells were subjected to indirect fluorescence microscopic observation. Calibration bar, 10 μm. (*B*) The hydrophilicity of CYP4F22 was analyzed by MacVector software (MacVector, Cary, NC) using the Kyte and Doolittle algorithm (window size, 15). (*C*) HEK 293T cells were transfected with pCE-puro 3xFLAG-CYP4F22, pCE-puro 3xFLAG-CYP4F22 (N-term, insertion of the *N*-glycosylation cassette to the N-terminus), pCE-puro 3xFLAG-CYP4F22 (E85/K, insertion of the cassette between Glu-85 and Lys-86), pCE-puro 3xFLAG-CYP4F22 (H155/R), pCE-puro 3xFLAG-CYP4F22 (A285/L), pCE-puro 3xFLAG-CYP4F22 (C361/R), pCE-puro 3xFLAG-CYP4F22 (D455/N), or pCE-puro 3xFLAG-CYP4F22 (R508/K). Lysates (3 μg) prepared from transfected cells were treated with or without endoglycosidase H (Endo H) and separated by SDS-PAGE, followed by immunoblotting with anti-FLAG antibodies. (*E*) Total cell lysates (10 μg) were centrifuged at 100,000 x g for 30 min at 4 ºC. The resulting supernatant (soluble fraction; S) and pellet (membrane fraction; M) were subjected to immunoblotting using anti-FLAG, anti-calnexin (membrane protein marker), or anti-GAPDH (soluble protein marker) antibodies. IB, immunoblotting. (*F*) HEK 293T cells transfected with plasmids encoding *3xFLAG-ELOVL4*, *3xFLAG-CERS3*, and *3xFLAG-*

CYP4F22 (wild type (WT) or *CYP4F22ΔN* (ΔN)), as indicated, were labeled with [^{3}H]sphingosine for 4 h at 37 °C. Lipids were extracted, separated by normal-phase TLC and detected by autoradiography. Cer, ceramide; GlcCer, glucosylceramide; SPH, sphingosine; SM, sphingomyelin; ω-OH, ω-hydroxy.

Fig. 5. CYP4F22 hydroxylates ULCFAs. (*A*) Keratinocytes were differentiated for seven days in the presence or absence of 10 μM fumonisin B_1. Lipids were extracted, treated with an alkali and derivatized to AMPP amides. Derivatized FAs were analyzed by a Xevo TQ-S LC/MS system and quantified by MassLynx software. Statistically significant differences are indicated (*p<0.05, **p<0.01; *t*-test). hC26:0 stands for hydroxy C26:0 FA. (*B*) Total membrane fractions (50 μg) prepared from BY4741 bearing the pAK1017 (vector) or pNS29 (*His$_6$-Myc-3xFLAG-CYP4F22*) plasmids were incubated with 10 μM C30:0 FA and 1 mM NADPH as indicated for 1 h at 37 °C. Lipids were extracted, derivatized to AMPP amides, and analyzed as in (*A*). The values represent the amount of each FA ω-hydroxylase activity relative to that of the vector/-NADPH sample. The value of the CYP4F22/+NADPH sample was statistically different from those of all other samples (**p<0.01; *t*-test). hC30:0 stands for hydroxy C30:0 FA. (*C* and *D*) HEK 293T cells were transfected with the plasmids encoding the indicated *ELOVL* (*ELOVL1* or *ELOVL4*), *CERS* (*CERS2* or *CERS3*), and *CYP4F22*. Transfected cells were labeled with [^{3}H]sphingosine for 4 h at 37 °C. Extracted lipids were separated by reverse-phase TLC (*C*) or by normal-phase TLC (*D*) and detected by autoradiography. Cer, ceramide; GlcCer, glucosylceramide; SPH, sphingosine; SM, sphingomyelin; ω-OH, ω-hydroxy.

Figure 1

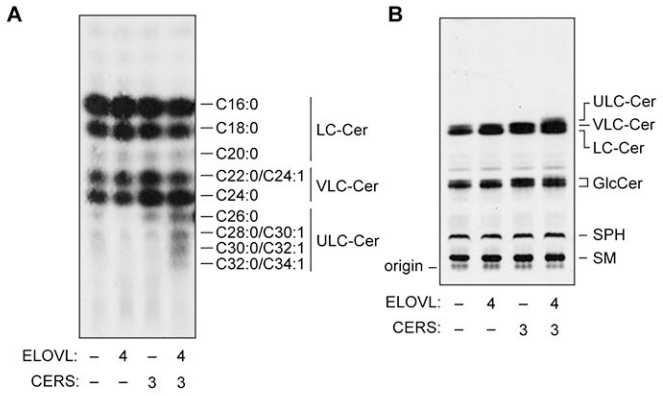
A
C16:0
C18:0
C20:0
C22:0/C24:1
C24:0
C26:0
C28:0/C30:1
C30:0/C32:1
C32:0/C34:1
LC-Cer
VLC-Cer
ULC-Cer
ELOVL: – 4 – 4
CERS: – – 3 3
B
ULC-Cer
VLC-Cer
LC-Cer
GlcCer
SPH
SM
origin
ELOVL: – 4 – 4
CERS: – – 3 3

Figure 2

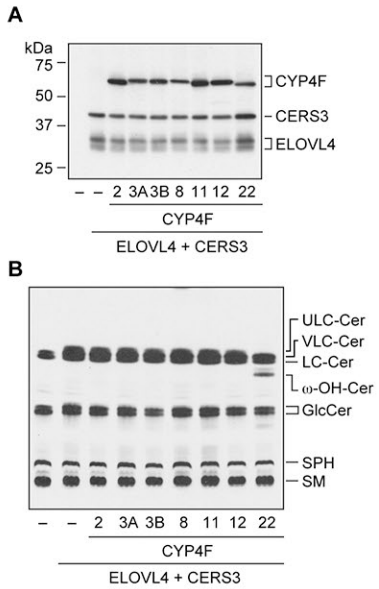
A
kDa
75
50
37
25
CYP4F
CERS3
ELOVL4
– – 2 3A 3B 8 11 12 22
CYP4F
ELOVL4 + CERS3
B
ULC-Cer
VLC-Cer
LC-Cer
ω-OH-Cer
GlcCer
SPH
SM
– – 2 3A 3B 8 11 12 22
CYP4F
ELOVL4 + CERS3

Figure 3

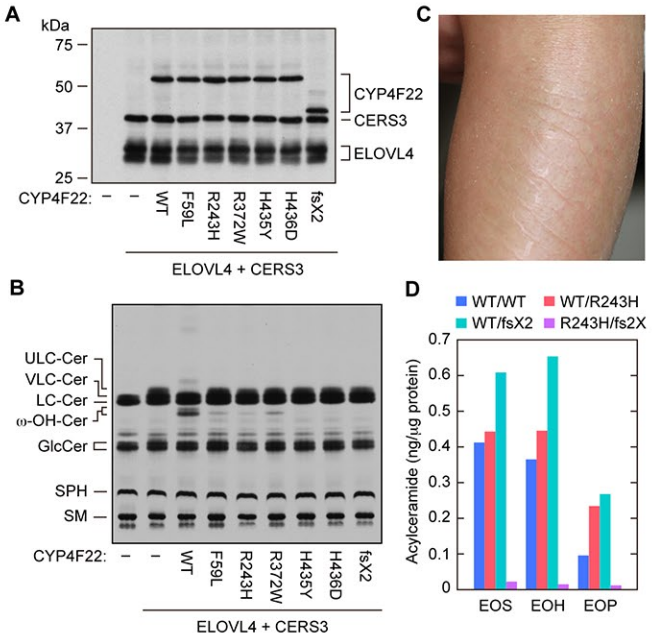
A
kDa
75
50
37
25
CYP4F22
CERS3
ELOVL4
CYP4F22: – – WT F59L R243H R372W H435Y H436D fsX2
ELOVL4 + CERS3
B
ULC-Cer
VLC-Cer
LC-Cer
ω-OH-Cer
GlcCer
SPH
SM
CYP4F22: – – WT F59L R243H R372W H435Y H436D fsX2
ELOVL4 + CERS3
C
D
WT/WT
WT/R243H
WT/fsX2
R243H/fs2X
Acylceramide (ng/µg protein)
0.7
0.6
0.5
0.4
0.3
0.2
0.1
0
EOS
EOH
EOP

Figure 4

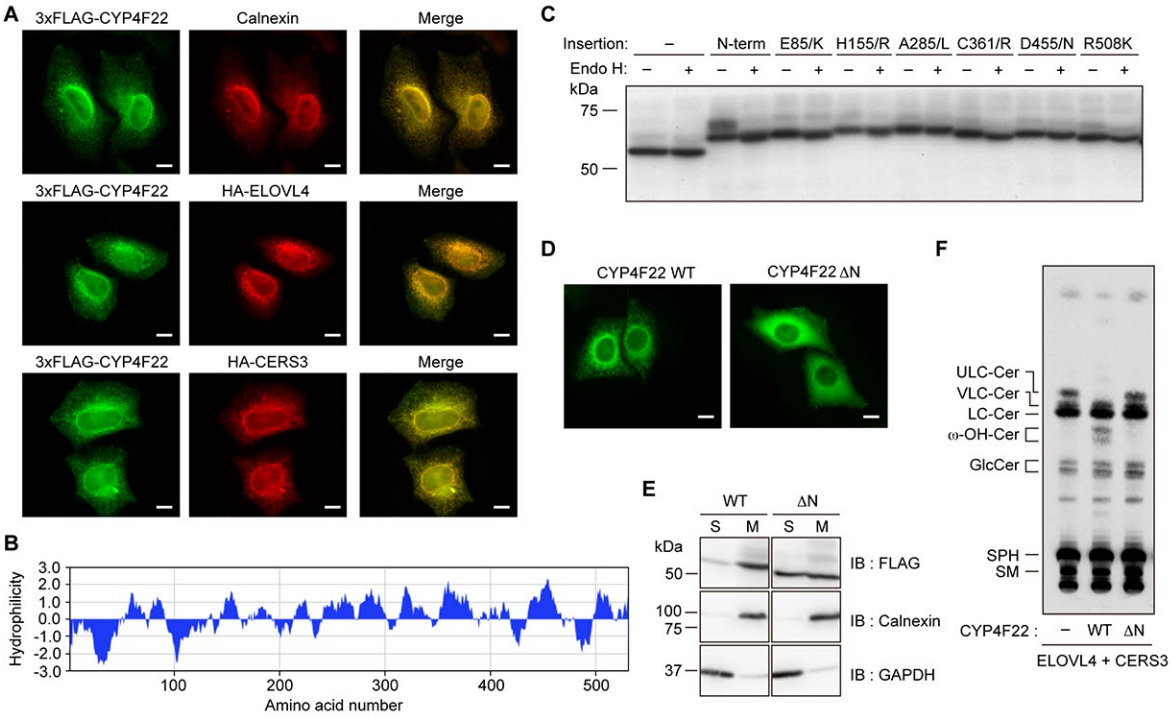
A
3xFLAG-CYP4F22
Calnexin
Merge
3xFLAG-CYP4F22
HA-ELOVL4
Merge
3xFLAG-CYP4F22
HA-CERS3
Merge
B
Hydrophilicity
3.0
2.0
1.0
0.0
-1.0
-2.0
-3.0
100
200
300
400
500
Amino acid number
C
Insertion: – N-term E85/K H155/R A285/L C361/R D455/N R508K
Endo H: – + – + – + – + – + – + – + – +
kDa
75
50
D
CYP4F22 WT
CYP4F22 ΔN
E
WT
ΔN
S M S M
kDa
50
100
75
37
IB : FLAG
IB : Calnexin
IB : GAPDH
F
ULC-Cer
VLC-Cer
LC-Cer
ω-OH-Cer
GlcCer
SPH
SM
CYP4F22 : – WT ΔN
ELOVL4 + CERS3

Figure 5

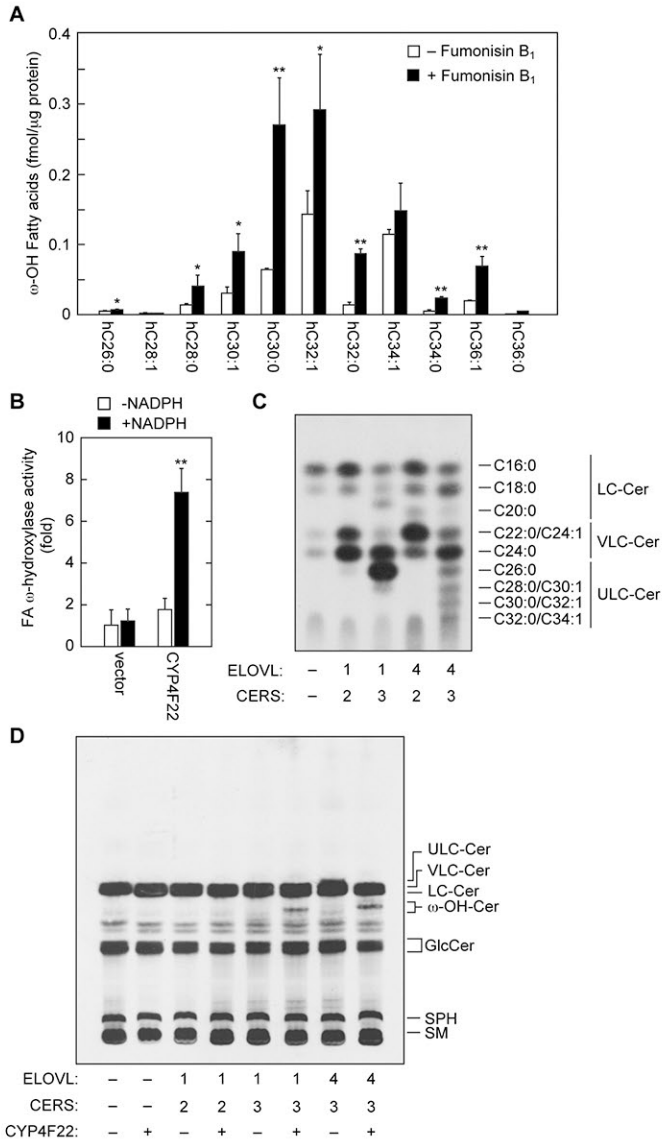
A
ω-OH Fatty acids (fmol/μg protein)
– Fumonisin B1
+ Fumonisin B1
hC26:0
hC28:1
hC28:0
hC30:1
hC30:0
hC32:1
hC32:0
hC34:1
hC34:0
hC36:1
hC36:0
B
-NADPH
+NADPH
FA ω-hydroxylase activity (fold)
vector
CYP4F22
C
C16:0
C18:0
C20:0
C22:0/C24:1
C24:0
C26:0
C28:0/C30:1
C30:0/C32:1
C32:0/C34:1
LC-Cer
VLC-Cer
ULC-Cer
ELOVL: – 1 1 4 4
CERS: – 2 3 2 3
D
ULC-Cer
VLC-Cer
LC-Cer
ω-OH-Cer
GlcCer
SPH
SM
ELOVL: – – 1 1 1 1 4 4
CERS: – – 2 2 3 3 3 3
CYP4F22: – + – + – + – +

Figure S1

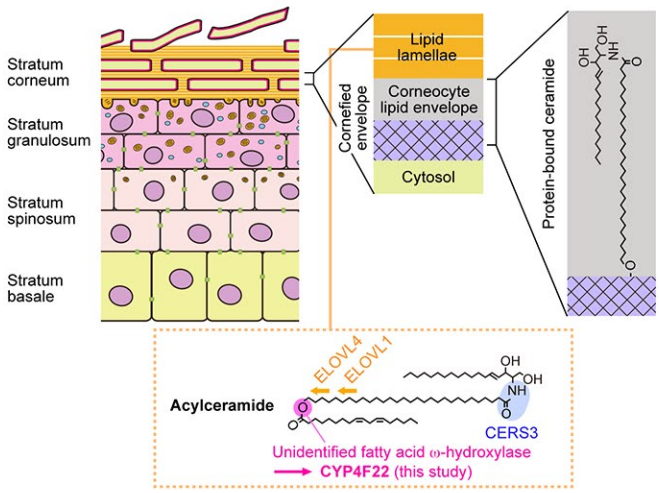
Stratum corneum
Stratum granulosum
Stratum spinosum
Stratum basale
Lipid lamellae
Corneocyte lipid envelope
Cornefied envelope
Cytosol
Protein-bound ceramide
Acylceramide
ELOVL4
ELOVL1
CERS3
Unidentified fatty acid ω-hydroxylase
CYP4F22 (this study)

Figure S2

A

LCBs \ FAs	Non-hydroxy FA [N]	α-hydroxy FA [A]	Esterified ω-hydroxy FA [EO]
Dihydrosphingosine [DS]	NDS	ADS	EODS
Sphingosine [S]	NS	AS	EOS
Phytosphingosine [P]	NP	AP	EOP
6-Hydroxysphingosine [H]	NH	AH	EOH

B

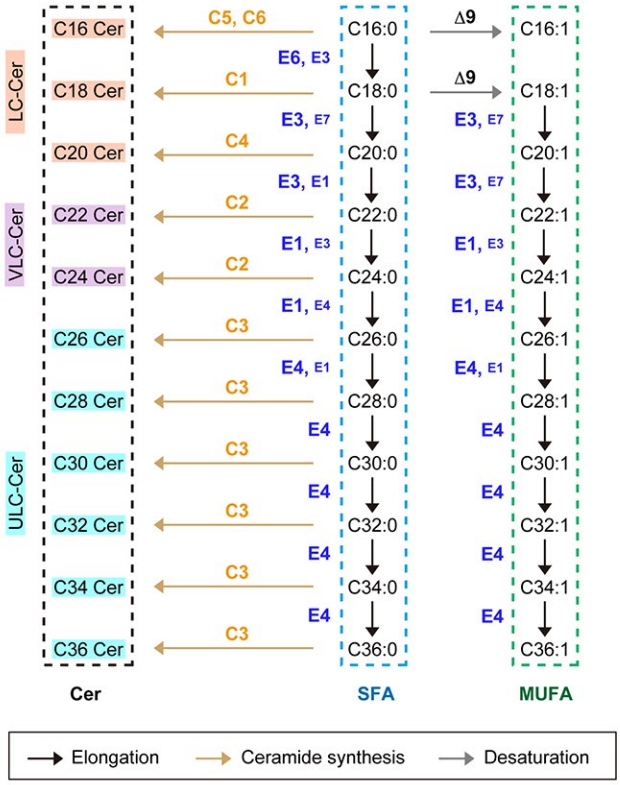

Figure S3

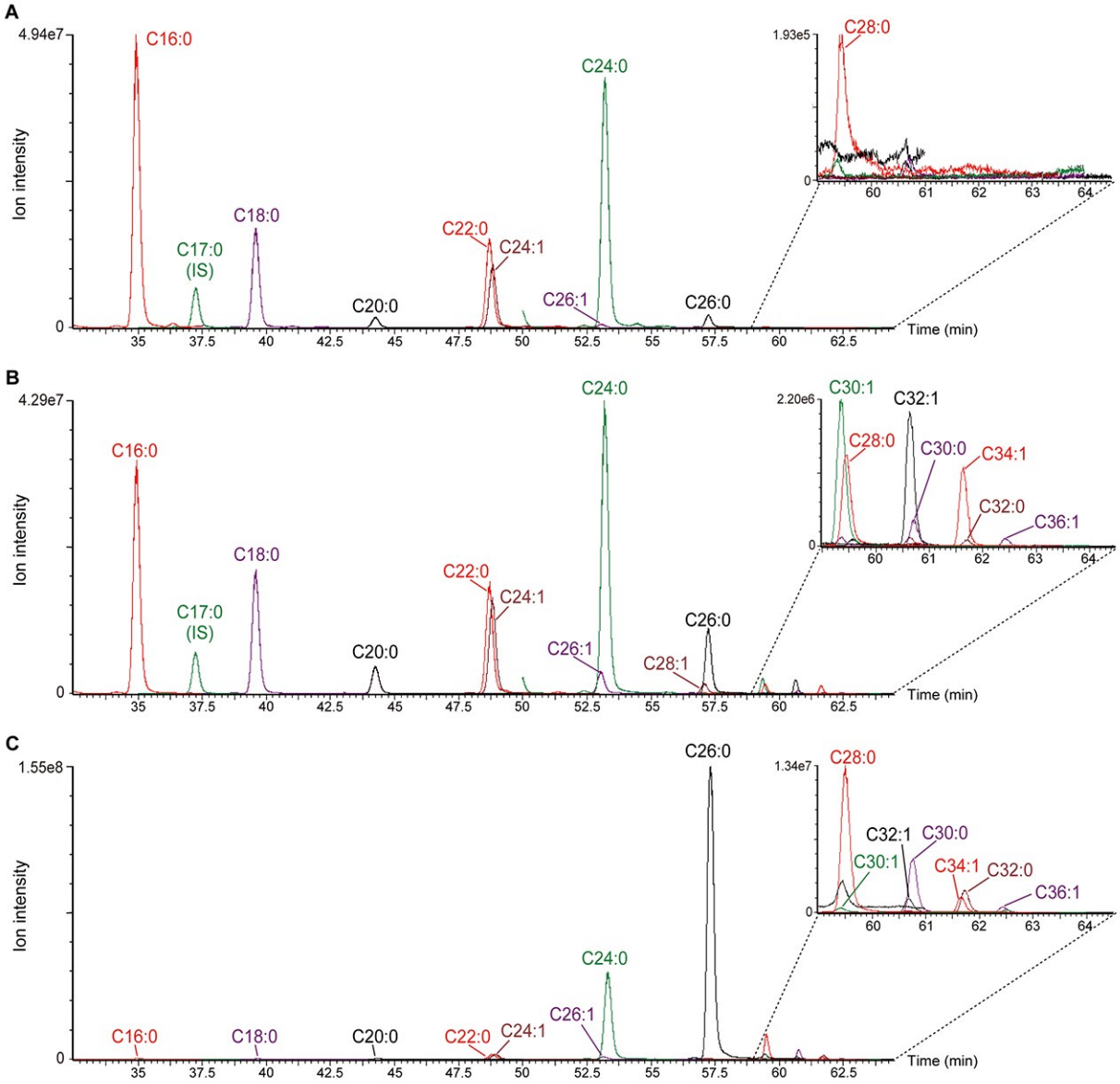
A
4.94e7
Ion intensity
C16:0
C17:0
(IS)
C18:0
C20:0
C22:0
C24:1
C24:0
C26:1
C26:0
Time (min)
1.93e5
C28:0
B
4.29e7
C16:0
C17:0
(IS)
C18:0
C20:0
C22:0
C24:1
C24:0
C26:1
C28:1
C26:0
2.20e6
C30:1
C32:1
C28:0
C30:0
C34:1
C32:0
C36:1
C
1.55e8
C16:0
C18:0
C20:0
C22:0
C24:1
C26:1
C24:0
C26:0
1.34e7
C28:0
C32:1
C30:0
C30:1
C34:1
C32:0
C36:1

Figure S4

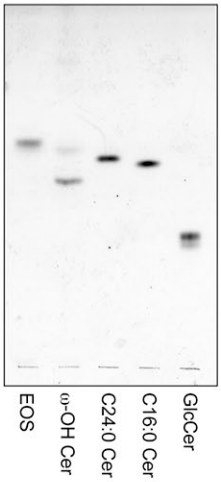

Figure S5

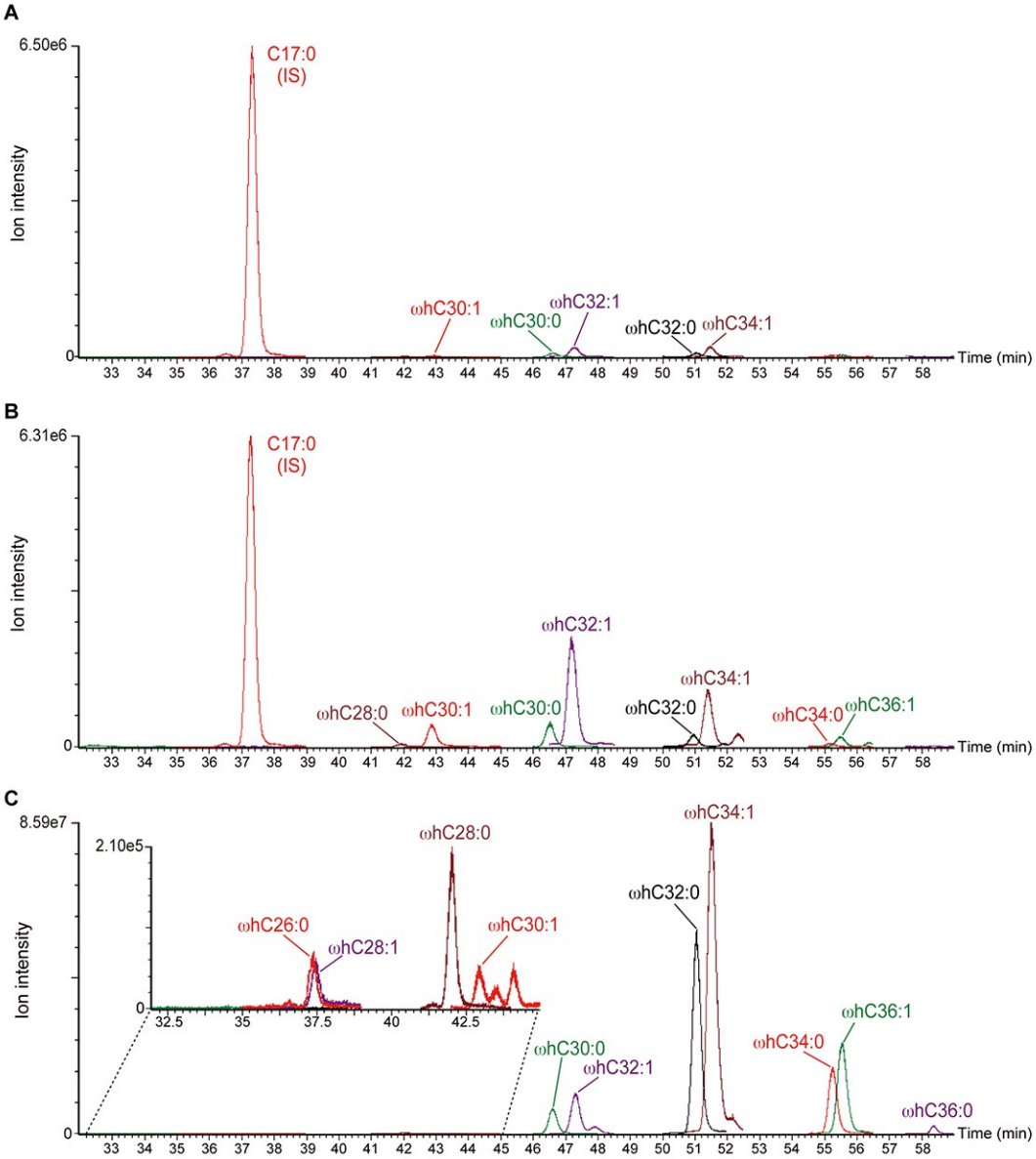
A
6.50e6
Ion intensity
0
C17:0
(IS)
ωhC30:1
ωhC30:0
ωhC32:1
ωhC32:0
ωhC34:1
Time (min)
B
6.31e6
Ion intensity
0
C17:0
(IS)
ωhC32:1
ωhC34:1
ωhC28:0
ωhC30:1
ωhC30:0
ωhC32:0
ωhC34:0
ωhC36:1
Time (min)
C
8.59e7
2.10e5
Ion intensity
0
ωhC28:0
ωhC34:1
ωhC32:0
ωhC26:0
ωhC28:1
ωhC30:1
ωhC36:1
ωhC34:0
ωhC30:0
ωhC32:1
ωhC36:0
Time (min)

Figure S6

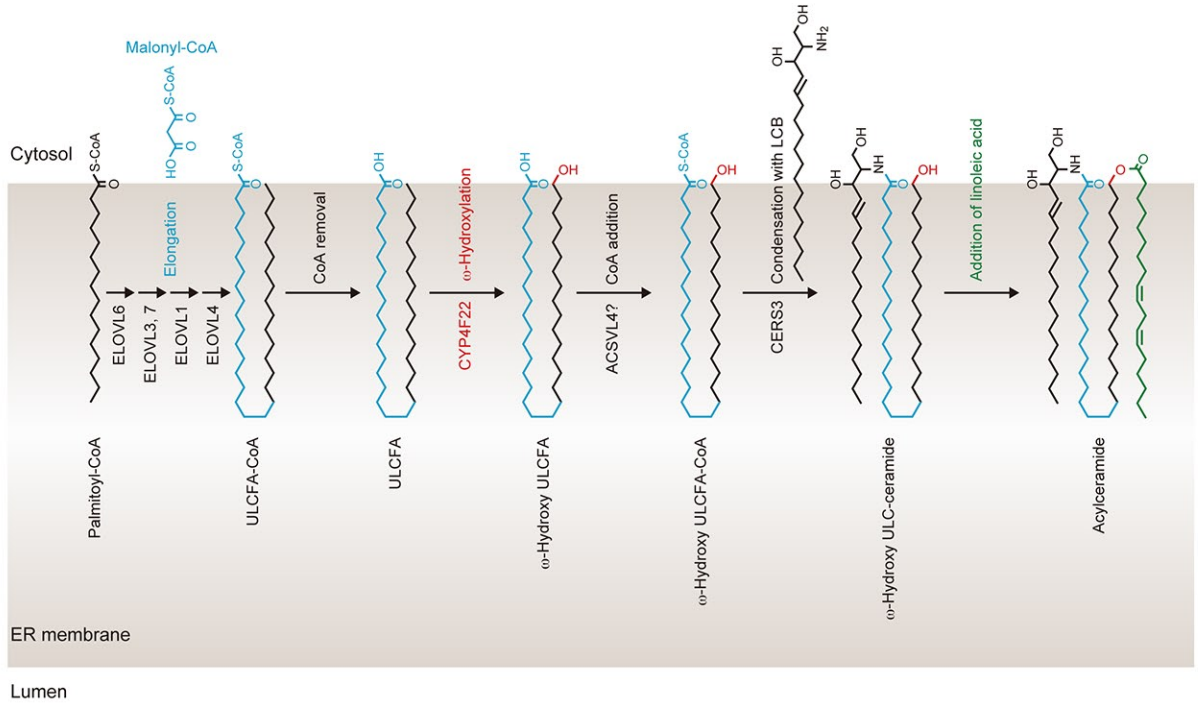
Cytosol
Malonyl-CoA
S-CoA
HO
O
Palmitoyl-CoA
ELOVL6
ELOVL3, 7
ELOVL1
ELOVL4
Elongation
ULCFA-CoA
CoA removal
ULCFA
OH
ω-Hydroxylation
CYP4F22
ω-Hydroxy ULCFA
ACSVL4?
CoA addition
ω-Hydroxy ULCFA-CoA
Condensation with LCB
CERS3
NH
NH2
ω-Hydroxy ULC-ceramide
Addition of linoleic acid
Acylceramide
ER membrane
Lumen